SCR-DeNOX Power Plant Design Optimization using HPC platforms: a Possible Automatic Workflow

R. Ponzini[1*], D. Feo, R. Pieri

[1] CINECA – via R. Sanzio 4 20090 Segrate (MI) Italy
e-mail: r.ponzini@cineca.it
e-mail:feodavide@gmail.com
e-mail: rpieri1988@gmail.com
corresponding author

Abstract

Selective catalytic reduction using ammonia is one of the most important industrial applications involved in NOx emissions reduction by means of filtering systems. The optimization of such systems is a complex problem mainly related to control of the fluid dynamics patterns right above to the filtering system present in the plant and driven by the correct definition of a set of angles of a set of turning vanes present upstream. Historically, this kind of optimization activity necessary to guarantee a limited pollution of the environment and preserve expensive filtering facilities ensuring longer life to vital parts of the energy production plant, was performed by means of experimental test bench coupled with some tailored computational model mainly used for a final verification of the selected optimal configuration. Today, thanks to the enormous improvement in computational modelling and computing facilities, this kind of activity can take advantage of using automatic, open-source tools and high-performance computing platforms to exploit a wider and autonomous analysis of the possible optimal configurations. Therefore, in this study, an automatic CFD optimization workflow has been developed for this kind of applications using open-source software on a selected practical case. The workflow is intended to autonomously evolve from a baseline plant CAD design to an improved one, modifying the angle of the turning vanes present in the model in order to decrease a quantitative synthetic index related to the level of uniformity of the velocity field distribution on the inlet section of the filtering system. The workflow designed is proven effective and able to autonomously decrease the selected index. Moreover, n the selected test case, the new design obtained shows an improved value of the target index of about 10%.

Keywords: Selective catalytic reduction, OpenFOAM, Dakota, HPC, optimization, CFD.

1. Introduction

Nitric oxides emission can cause problems to airways and damage the environment, being the mainly responsible for photochemical pollution (see Institute of Clean Air Companies 1997 and 200). It is thus very important to control them. Available technologies to reach this goal are divided into two categories:

1. primary control technologies, like low-NOx burners (high efficiency burners) or Over Fire Air, which limit temperature to reduce NOx production. This technology has an efficiency up to 50%;

2. secondary control technologies, which reduce NOx presence in exhaust gas. They are divided in two more categories:

   a. Selective non-catalytic reduction, which works at high temperatures (1000°C) and has an efficiency up to 65%;

   b. Selective catalytic reduction. In this case, the presence of a catalyst allows to work at low temperatures (350°C) and have efficiency up to 95%.

Efficiency can be calculated thanks to this formula (Xu et al. 2013):

$$\mu = 100 \frac{(c_{in}-c_{out})}{c_{in}} \tag{1}$$

where C_{in} and C_{out} are concentrations of NOx at the inlet and at the outlet of the duct.

Standard SCR-DeNOx plants are very complex, presenting in general many geometrical components including:

- an *ammonia injection grid* (AIG) to inject ammonia in the flow;

- a *hybrid grid* to generate turbulence for a better mixing;

- a set of *turning vanes* to direct the flow through the corners and guarantee uniform flow at catalyst entrance;

- a *straightener* before the catalyst layers;

- a *catalyst layers* where exothermal chemical reactions take place.

The main chemical reactions taking place in the catalyst are:

$$4NH_3 + 4NO + O_2 \rightarrow 4N_2 + 6H_2O \tag{2}$$

$$4NH_3 + 2NO_2 + O_2 \rightarrow 3N_2 + 6H_2O \tag{3}$$

$$NO + NO_2 + 2NH_3 \rightarrow 2N_2 + 3H_2O \tag{4}$$

The first reaction (Equation 2) is the most important one. Actually, 95% of nitric oxides in the duct is made of NO. Due to the complexity of these plants, in order to perform an optimization, it is possible to focus on many different design perspectives. For example, it is important to design an AIG able to maximize mixing between ammonia and exhaust gas. Another important objective is to avoid particulates sediment along the duct adding entrapment boxes.

In this study, the main goal is to focus on the fluid dynamics patterns present in the power plant and perform an optimization designed to obtain a uniform flow distribution at catalyst entrance (see Xu et al. 2013 and Xu et al. 2014). In fact, lack of uniformity of the velocity field at catalyst entrance is very important for many reasons:

- power plant efficiency reduction;

- unreacted ammonia released in atmosphere;

- catalysis failure corresponding to velocity peaks.

To drive the flow uniformity on the catalyst inlet surface, it is possible to arrange the relative orientation angle of the *turning vanes* positioned upstream the catalyst neglecting both

the thermodynamics effects and the chemical reactions present in the real physics of this kind of power plant (see Xu et al. 2013 and Xu et al. 2014).

Historically, this kind of optimizations were performed by means of experimental test bench, usually built in a reduced scale keeping valid some fluid dynamics equivalence, coupled with some tailored computational model mainly used for a final verification of the selected optimal configuration. Today, thanks to the enormous improvement in computational modelling and computing facilities, this kind of activity can take advantage of using automatic and open-source tools and high-performance computing platforms to exploit a wider and automatic analysis of the possible optimal configurations. Therefore, in this work, an automatic optimization workflow fully based on 3D computational fluid dynamics (CFD) has been designed and developed for this kind of applications using open-source software. The workflow is intended to autonomously evolve from a baseline plant CAD design to an improved one, modifying the angle of the turning vanes present in the model in order to decrease a quantitative synthetic index related to the level of uniformity of the velocity field distribution on the inlet section of the filtering system. To evaluate velocity field uniformity, it is possible to define a quantitative index named *relative standard deviation* (as shown in Xu et al. 2013 and Xu et al. 2014) and defined as*:*

$$RSD \ = \ \frac{\sqrt{\sum_{i=1}^{n}(u_i - U_{avg})^2}}{(n-1)^{0.5} \cdot U_{avg}} \tag{5}$$

where u_i is the velocity corresponding to *i-th* CFD mesh cell, U_{avg} is the average velocity at catalyst entrance and n is the number of mesh cells used to discretize the catalyst entrance surface. The workflow designed is proven to be effective and able to autonomously decrease the selected index. Moreover, for the selected test case, the new design obtained shows an improved value of the target index of more than 12%.

The forthcoming of the paper is organized in the following way:

- in Section 2, the computational approach defining the CAD design is selected, the set of Equations solved and the meshing strategy presented,

- the workflow automation on HPC systems describing the open-source tools is used and the way they are connected into a single automatic procedure is discussed in Section 3,

- the main results including the comparison between the starting and the optimized design are shown in Section 4,

- discussion of main results and possible future work are addressed in Section 5.

2. Computational approach

In Figure 1a, the simplified geometry chosen in our study include these geometrical elements:

- ammonia injection grid (AIG), in green;

- turning vanes (in orange and violet);

- catalyst layer (in yellow);

- inlet and outlet are tagged in blue and red, respectively.

The air schematic flow pattern is present in Fig. 1b using the blue arrows. AIG is positioned upstream the first corner and it consists of 11 evenly spaced cylinders, whose

diameter is 8 mm. Turning vanes are made of two lines of plates with negligible thickness and they are modeled as no-thickness baffles. The first row is made of four baffles whereas the second row is made of six baffles. The real physical problem is multi-physical and very complex. In the literature, the model chosen for the solution in simpler (see Xu et al. 2013 and Xu et al. 2014). More in detail, unsteadiness, heat transfer and chemical reaction are considered as negligible at first and only turbulence and pressure drop corresponding to the catalyst are considered. The fluid dynamics problem considered was therefore modeled as a steady state 3D turbulent one. Under this configuration, the fluid dynamics problem is defined by the set of Navier-Stokes equations where the catalyst, positioned downstream the last corner, is modeled as a porous media. The pressure drop corresponding to the catalyst layer is calculated through *Darcy* law and the coefficients are chosen to obtain a drop of 130 Pa (according to Xu et al. 2013 and Xu et al. 2014). For the solution, the so-called Reynolds Averaged Navier Stokes (RANS) simulation approach (see Reynolds 1895) was chosen. RANS simulations are recognized to be the standard de-facto in industrial applications allowing to account for the complexity of turbulent fluid dynamics using mesh size that is manageable by modern hardware in a few hours. Nevertheless, RANS modelling requires the definition of an additional set of equations, the so-called closure equations, necessary to emulate the dissipation of the turbulent energy within the problem. In this case, we selected a two-equations turbulence model called *kw-SST* turbulence model since it is recognized to perform very well in adverse pressure gradients and separating flow conditions (see Menter 1993 and 1994). This kind of physics has been modeled using the open-source CFD toolbox OpenFOAM (see openFoam User Guide).

The boundary conditions and the initial conditions were set according to the working conditions of the power plant. For the velocity field, a value of 4 m/s was chosen with a uniform profile at inlet and a no-slip condition at walls. At outlet, the velocity field is not constrained. For the pressure, a uniform zero pressure was chosen at outlet. At walls and inlet, the value is computed, not constrained, and set as reference at zero.
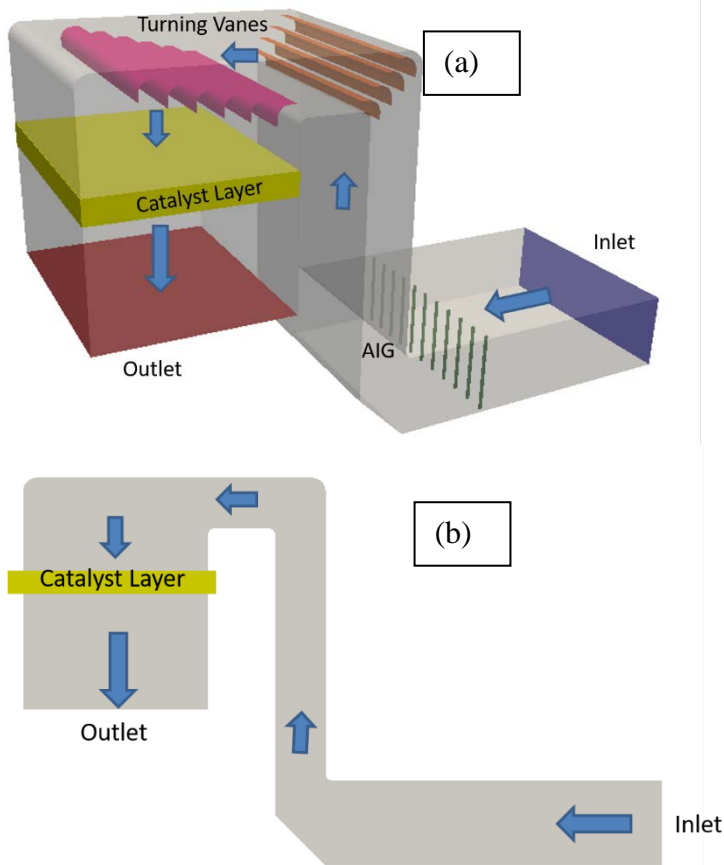
Fig. 1. (a) Iso-metric view of the power plant simplified geometry, components and flow
pattern; (b) Side view of the power plant simplified geometry and flow pattern

The meshing procedure was performed using standard OpenFoam meshing utilities, *blockMesh* and *snappyHexmesh*. These tools allow the user to create hexa-dominant high quality 3D CFD meshes enabling a fine control of mesh cell size spacing and of the boundary layer thickness. In Fig. 2, a snapshot of the mesh obtained for a generic configuration is given. Notably, in correspondence to the wall boundaries, a boundary layer buffer is defined to ensure proper solving of the equation. The average mesh size for this problem consists of about 4.5 million cells.
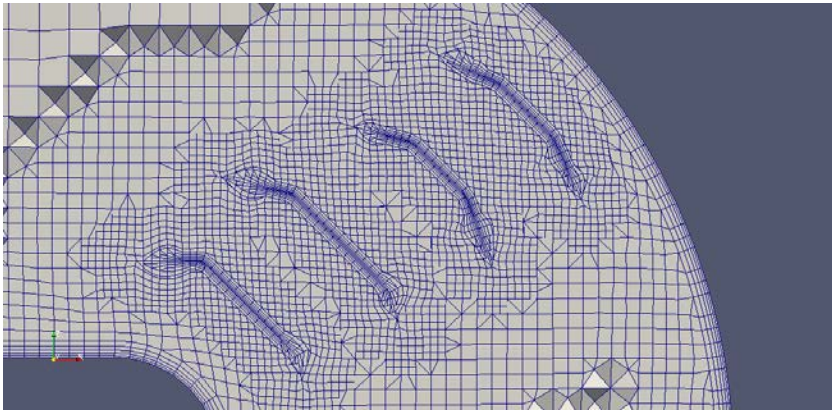
Fig. 2. Mesh sample

The CFD simulations are performed on the CINECA hardware, a *IBM NeXtScale*, made of 516 computational nodes, each node equipped with 2 8-cores Intel Haswell 2.40 GHz core, for a total of 16 cores/node and a RAM of 128 GB/node. The internal Network is an *Infiniband* with 4xQDR switches. Thanks to this kind of computational facility, the single CFD run takes about two hours to get a convergent solution using 32 computational cores.

For the reference simulation, the geometry presented in Fig. 1 was used. The computation was performed selecting a uniform profile velocity field at inlet, choosing a value of 4 m/s as discussed above. At outlet, a condition of zero pressure was chosen. In Fig. 11, it is possible to see the pressure field along the duct. You can notice a localized pressure-drop corresponding to the catalyst activity as set according to Darcy's law. The resulting flow patterns for both pressure drops and velocity distribution obtained are shown in Fig. 3 for the baseline CAD design.
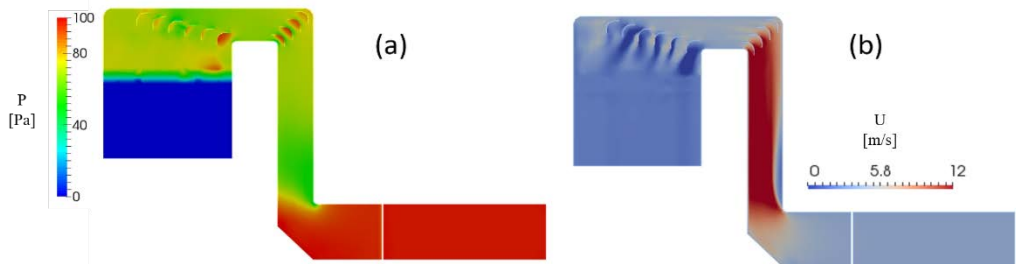

Fig. 3. Baseline CFD results: (a) Pressure distribution; (b) Velocity distribution

3. Workflow automation

The central point of this study is the automation procedure. The standard CFD workflow can be in fact automated and used to perform optimization thanks to standardization of CAD management, the meshing procedure and the post-processing of data and thanks to the usage of templates for the solving procedure. As shown in Fig. 4, the optimization is performed acting on the angles of attack of the turning vanes as input parameters for the single CFD run while the output is represented by the *RSD* value as defined by Eq. 5 in Section 1.
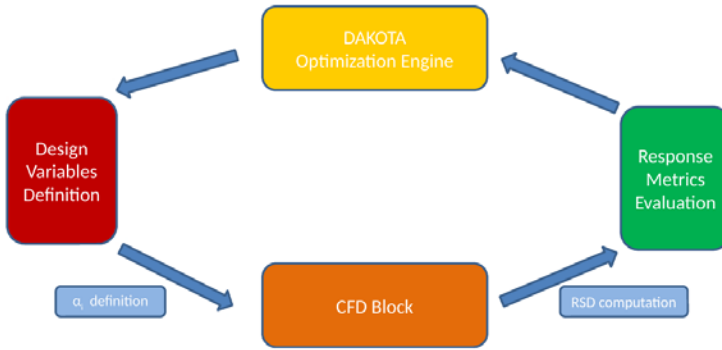
Fig. 4. Automatic workflow scheme. The optimization engine is Dakota (yellow box), the angle of attack of the turning vanes are the optimization variables, the parameter to be optimized is the RSD value computed at the filter entering surface. All the CFD runs, from mesh generation to data post-processing are automatic (orange box)

Nevertheless, this process can be autonomously performed only if the single CFD block defined for each novel configuration of the turning vanes as defined by the optimization process is able to run without any external intervention. In Fig. 5, it is possible to see the diagram of the set of steps that have been standardized and automated relative to a single CFD block. The single CFD block consisting of six main steps:

1. acquiring of the CAD base-line (reference geometry);

2. definition of the turning vanes rotation values;

3. update the CAD with novel turning vanes position;

4. generation of a valid mesh;

5. computation of the fluid dynamics solution;

6. post-process data and RSD evaluation.

The automation process of the standardized CFD block is performed using the Python programming language and a set of standard file format including the stereolithography (STL) for CAD description and the visualization toolkit (VTK, (see Schroeder et al.)) for data output. Both these kind of file formats are supported by OpenFOAM standard utilities and are therefore easily managed.
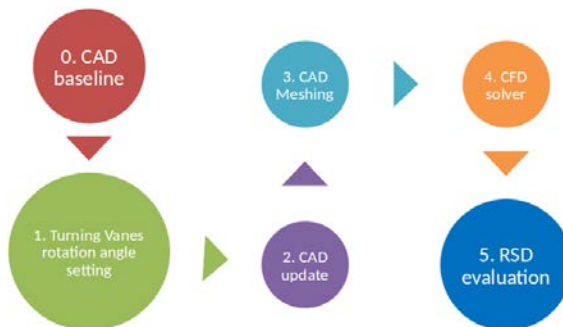

Fig. 5. Single automatic CFD block

The open-source software Dakota (see Dakota User Manual) manages the optimization engine. This open-source software is able to use many different optimization algorithms. In this case, we are facing an unconstrained optimization and we therefore select a gradient-based method. The selected algorithm is very efficient and it is advantageous in terms of computational costs. The gradient-based method solves a number of sub-problems consisting of minimizing a quadratic function in a space defined by the gradient. Search directions are conjugated to the Hessian. In Dakota different methods to compute it are implemented, and we select the Fletcher-Reeves method (see Hestenes et al. 1952). For our test, in one optimization loop, it was possible to test about 60 different geometrical configurations at a time in 24 hours. Concurrency of multiple CFD runs is an entry parameter for the Dakota optimization driver that can be tuned to allow Dakota to submit a desired number of CFD runs at a time. Nevertheless, the key strategy to enable multiple CFD solutions at a time are the availability of an HPC platform and the choice of open-source building blocks. In fact, on one hand, without a large availability of computational resources each next CFD computation must wait until the end of the previous one is reached, but on the other hand, this would not be sufficient since a license-based CFD solver would limit the actual number of concurrent CFD runs. This kind of approach, proven here to be robust and reliable, would be a novel valuable tool usable in the early design stage of this kind of expensive and complex energy plants.

4. Results

The main result of this study is the autonomous improvement of the RSD value for the selected test case that show a clear decreasing pattern from a starting value of about 54%, which indicates great non-uniformity in the velocity field, to a value of less than 45% as shown in Fig. 6. These changes can be related to a great improvement in the overall efficiency of the power plant and to a specific improvement in the efficiency of the chemical reactions at the catalyst surface thus limiting the presence of unreacted ammonia in the outgoing fluid flow.
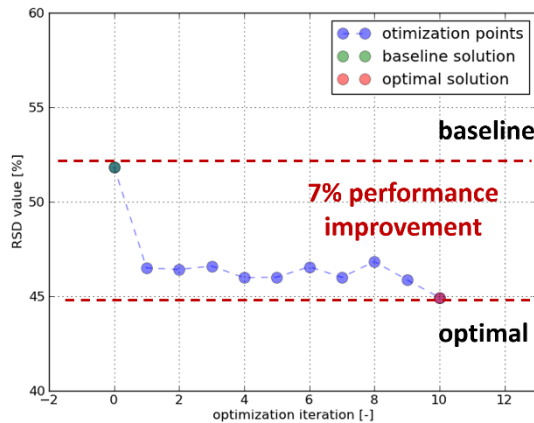

Fig. 6. Optimization pattern for the RSD value

The value of the RSD index is coherent to improved fluid dynamics of the catalyst inlet surface. Figure 7 shows the local distribution of the velocity values on the catalyst inlet surface for the two designs: on the left, the baseline design is shown whereas on the right, the improved optimal design is given. Notably, the velocity peak is strongly reduced ensuring a more uniform distribution and thus decreasing the risk of catalyst failures.
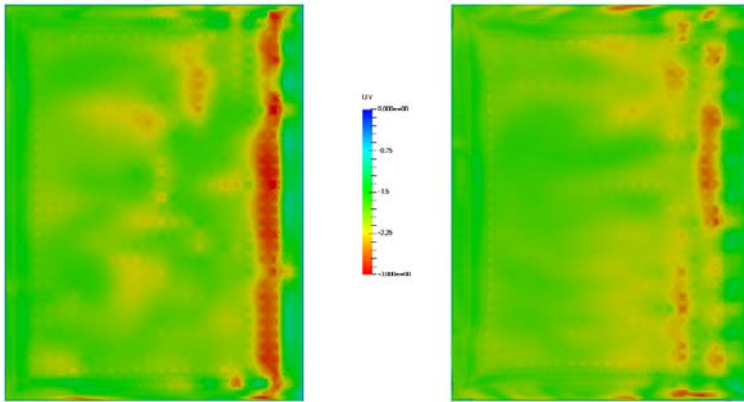
Fig. 7. Velocity field at catalyst entrance for the baseline design (left) and for the optimized design (right).

Moreover, from the automation point of view, it is relevant to underline that the optimization process is able to evolve autonomously under a wide range of starting conditions and using different ranges to explore the turning vanes allowed angles. In all our tests, the workflow was able to reach the end of the search pattern without any failure.

5. Conclusions and future work

The results presented herein suggest that the automatic designed workflow works properly. By activating the rotation of turning vanes in the first corner upstream the catalyst, we obtained a reduction of the targeted RSD value of about 10%, reducing its value from 54% to 44%. Accordingly, the higher velocity-peak area is considerably reduced after the optimization process, decreasing the risk of catalyst failures. This main result of the study is per-se relevant but it became even more relevant if we consider that it has been obtained in an automatic way by the workflow starting from the reference configuration and moving separately each raw of the turning vanes wondering to reduce the value of the selected synthetic index. Nevertheless, RSD value remains rather high and a big recirculation area in the last corner can be noticed. These two problems are probably due to a separation in the first corner of the power plant selected design, persisting along the whole duct. Unfortunately, it is not possible to modify the walls geometry so some turning vanes should be added in the first corner to limit the problem. Looking at the RSD definition, some specifications must be done. RSD value is calculated using point values of the velocity field. The grid is much more refined near the wall than in the duct center. In this way, the near-wall region has a much higher weight in the RSD computation. It would be worth creating a window to rule out the near-wall region from RSD computation. Furthermore, another important feature in this problem is the orientation of the flow approaching the catalyst. To take account of this, it should be possible to define a RSD for the flow angles at catalyst entrance and operate a multi-objective optimization. In conclusion, the automated workflow proved to be effective on a real life test case, giving encouraging results. It would be interesting to define more powerful objective functions and operate multi-objective optimizations to take into account different aspects of the problem. Furthermore, Dakota gives the possibility to use many different optimization algorithms and it would be worth comparing their performances with respect to our choice. It is worth to point out that gradient-based optimization methods are highly efficient, with the best convergence rates of all

of the optimization methods since they look for improvement based on derivative information and are a clear choice when the problem is smooth, unimodal, and well-behaved. However, when the problem exhibits a non-smooth, discontinuous, or multimodal behavior, these methods can also be the least robust since inaccurate gradients will lead to bad search directions. The procedure showed herein is only a proof of concept; a more generalized version of the study should be implemented in order to allow other researchers to use it. For this reason, the automation scripts and input files are not available for public download.

Acknowledgements

References

CINECA hardware, http://www.hpc.cineca.it/hardware/galileo
CINECA ISCRA grant, http://www.hpc.cineca.it/services/iscra
Dakota User's Manual. https://dakota.sandia.gov/documentation.html
Hestenes MR, Stiefel E (1952). Methods of Conjugate Gradients for Solving Linear Systems. *Journal of Research of the National Bureau of Standards*, 49, 6.
Institute of Clean Air Companies (1997). White paper: Selective catalytic reduction (SCR) control of NOx emissions. Washington, DC: Institute of Clean Air Companies Inc.
Institute of Clean Air Companies (2000). White paper: Selective non-catalytic reduction (SNCR) for controlling NOx emissions. Washington, DC: Institute of Clean Air Companies Inc.
Menter FR (1993). Zonal Two Equation k-ω Turbulence Models for Aerodynamic Flows, *AIAA Paper* 93-2906.
Menter FR (1994). Two-Equation Eddy-Viscosity Turbulence Models for Engineering Applications, *AIAA Journal*, 32, 8, 1598-1605.
OpenFOAM User Guide. http://www.openfoam.com/documentation/user-guide/
Reynolds O (1895). On the Dynamical Theory of Incompressible Viscous Fluids and the Determination of the Criterion. *Philosophical Transactions of the Royal Society of London*. A, 186, 123-164.
Schroeder W, Martin K, Lorensen B (2006). *The Visualization Toolkit* (4th ed.), Kitware, ISBN 978-1-930934-19-1
YuanYuan X, Yan Z, Fengna L, Weifeng S, and JingQi Y (2014). CFD analysis on the catalyst layer breakage failure of an scr-denox system for a 350 mw coal-fired power plant. *Computers and Chemical Engineering*, 69:119–127.
YuanYuan X, Yan Z, Jingcheng W, and JingQi Y (2013). Application of CFD in the optimal design of a scr-denox system for a 300 mw coal-fired power plant. *Computers and Chemical Engineering*, 49:50–60.